

RSC Advances

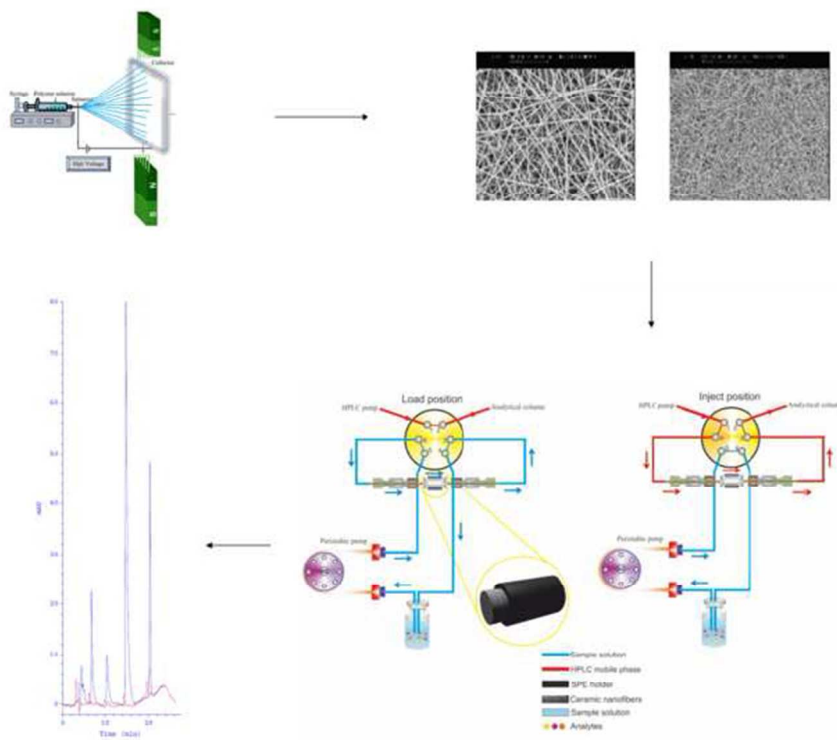


This is an *Accepted Manuscript*, which has been through the Royal Society of Chemistry peer review process and has been accepted for publication.

Accepted Manuscripts are published online shortly after acceptance, before technical editing, formatting and proof reading. Using this free service, authors can make their results available to the community, in citable form, before we publish the edited article. This *Accepted Manuscript* will be replaced by the edited, formatted and paginated article as soon as this is available.

You can find more information about *Accepted Manuscripts* in the [Information for Authors](#).

Please note that technical editing may introduce minor changes to the text and/or graphics, which may alter content. The journal's standard [Terms & Conditions](#) and the [Ethical guidelines](#) still apply. In no event shall the Royal Society of Chemistry be held responsible for any errors or omissions in this *Accepted Manuscript* or any consequences arising from the use of any information it contains.



190x148mm (96 x 96 DPI)

1 **Magnetic and electric fields assisted electrospun polyamide nanofibers for on-line μ -**
2 **solid phase extraction and HPLC**

3 Habib Bagheri*, Hamed Piri-Moghadam, Soroush Rastegar

4 *Environmental and Bio-Analytical Laboratories, Department of Chemistry, Sharif University of*
5 *Technology, P.O. Box 11365-9516, Tehran-Iran*

6 **Abstract**

7 The effects of applied magnetic and electric fields in electrospinning were investigated to produce
8 more efficient nanofibers. Considering the previous extensive studies, polyamide nanofibers were
9 prepared by conventional approach and under auxiliary electric and magnetic fields. The first
10 sorbent was synthesized by electrospinning of a solution of 18% polyamide in formic acid. The
11 second and third types of polyamide were prepared similarly while the electrospinning processes was
12 assisted by an electric and a magnetic field, respectively. The third type of polyamide contained
13 magnetic ionic liquid (MIL) to induce sufficient magnetic susceptibility to the polymeric solution.
14 The SEM images revealed that the application of auxiliary electric and magnetic fields led to the
15 aligned nanofibers with mean diameters of 200 and 90 nm, respectively while for the conventional
16 electrospun non-woven nanofibers the mean diameter was 500 nm. To evaluate the extraction
17 efficiency of the prepared nanofibers, they were removed from the collector electrode and packed
18 into the μ -solid phase extraction (μ -SPE) cartridge, coupled on-line with high performance liquid
19 chromatography (HPLC). Apart from the influence of the assisted fields on electrospinning, the
20 effects of size of the nanofibers and the ionic liquid content on the μ -SPE of imidacloprid,
21 metribuzin, ametryn and chlorpyrifos were investigated. The highest extraction efficiency was
22 achieved for the third sorbent due to its higher aspect ratio. After preparation of five sets of
23 nanofibers, it was revealed that the presence of MIL dopant up to 10 % in a solution of 18%
24 polyamide exhibited the most satisfactory results. The linearity for the analytes was in the range of

*Corresponding author. Tel.: +98-21-66165316; Fax: +98-21-66012983
E-mail address: bagheri@sharif.edu (H. Bagheri)

25 1–500 $\mu\text{g L}^{-1}$. Limit of detection (LOD) was in the range of 0.4–4 $\mu\text{g L}^{-1}$ and the RSD% values (n
26 = 5) were all satisfactory at the 20 and 200 $\mu\text{g L}^{-1}$ levels. The applicability of the developed on-line
27 μ -SPE-HPLC method was examined by analyzing real water samples obtained from spiked
28 Zayandeh rood river and Caspian Sea and the relative recovery percentages were from 84 to 108%
29 at 20 and 200 $\mu\text{g L}^{-1}$ levels.

30 *Keywords: Auxiliary electrode electrospinning, magnetic field assisted electrospinning, magnetic*
31 *ionic liquids, on-line μ -SPE-HPLC*

32

33

34 1. Introduction

35 With the rise of worldwide trade in agricultural products in recent years, researchers are paying
36 more attentions to the development of novel analytical techniques to monitor the pesticides
37 residues in drinking waters. Pesticides, including insecticides, acaricides, fungicides, and
38 herbicides usually present at trace levels throughout the whole environment. There is therefore
39 a need to develop sensitive methods for their determination. Solid phase extraction (SPE) is a
40 popular and well-established sample preparation method used for isolation, enrichment and/or
41 clean-up of components of interest from aqueous samples [1]. The solid phase sorbent is
42 usually packed into small tubes or cartridges. Recently many developments in this technology
43 have taken place including new formats such as discs, pipette tips, 96-well plates and μ -SPE
44 [2-5]. Preparation of new sorbents such as silica or polymer-based media and mixed- media has
45 been also focused for several years. Synthesizing the new sorbents, however, has remained a
46 challenging task towards preparing homogenous sorbents with improved aspect ratios.

47 Electrospinning is a versatile method for the production of nonwoven fibers ranging in size
48 from nano to micro scale. Therefore, it has been adopted in various fields of science tissue
49 engineering, energy storage, sensors and environmental engineering [6]. Electrospun
50 nanofibers were recently applied for extraction of desired analytes by μ -SPE and solid phase
51 microextraction [7-9]. A wide range of polymers, composites, and ceramic precursor solutions
52 have been electrospun into non-woven fiber mats. Sometimes electrospinning is followed by
53 secondary operations, such as heat treatment or coating the previously electrospun fibers [10].
54 The primary setup for electrospinning includes a spinneret with a metallic needle, a high
55 voltage power supply, and a grounded collector. Many processing parameters affect the fiber
56 diameter, such as distance between needle and collector, polymer flow rate, and the applied
57 voltage. By changing the primary electrospinning set up, the construction and morphology of

58 the electrospun nanofibers can be altered. Electrospun fibers are randomly pointed and form
59 nonwoven mats while for broader applications of electrospinning it is desirable to generate
60 periodic or organized structures from nanofibers. There have been a few approaches to make
61 well aligned nanofibers by electrospinning [11-15]. Increasing the rotational speed of the
62 collecting drum, introducing a potential across a gap or series of gaps in the collecting
63 electrode, introducing an external lens element or a viscous liquid environment, or rapidly
64 oscillating a grounded frame within the liquid jet are some typical examples. All of these
65 methods rely on minimizing the fiber instability by applying external forces on the fibers
66 during production. Yang et al. [16] also reported an approach for fabrication of well-aligned
67 arrays and multilayer grids by a method called magnetic electrospinning (MES). In MES, the
68 polymer solution is magnetized by the addition of a small amount of magnetic nanoparticles.
69 The solution is electrospun into fibers while a magnetic field generated by two parallel-
70 positioned permanent magnets is applied. The magnetic field stretches the fibers across the gap
71 to form a parallel array as they land on the collector. An aluminum foil collector is placed
72 between the magnets and acts as the cathode. The length of the distance between the magnets
73 could be changed from several millimeters to several centimeters, which determines the width
74 of the resultant arrays.

75 Ionic liquids (ILs) are non-molecular solvents that have captured the interest of many in
76 academics and are currently being introduced into a number of industrial processes worldwide
77 [17,18]. Ionic liquids (ILs) are increasingly being used in analytical chemistry [19-22]. It has
78 been recently used as the sorbent in microextraction techniques [23]. ILs could be easily
79 magnetized and used as the active reagent of polymer solution for MES.

80 In here, the effects of electric and magnetic fields as well as the IL content on the morphology and
81 structure of the electrospun nanofibers were investigated *via* the on-line μ -SPE-HPLC of
82 imidacloprid, metribuzin, ametryn and chlorpyrifos. Auxiliary electrode electrospinning (AE) and

83 magnetic field assisted electrospinning (MFAES) led to the reduction of the nanofibers diameters.
84 The obtained data revealed that all nanofibers have great potential for the trace enrichment purposes.
85 The nanofibers mat prepared by MFAES was selected for further analysis and validation due to its
86 highest extraction efficiency. While the effect of MIL was also investigated, the relative recoveries
87 proved the ability of the prepared sorbent for analysis of the selected analytes in the river and sea
88 samples.

89

90

91 **2. Experimental**

92

93 **2.1. Instrument**

94 A Knauer (Berlin, Germany) HPLC system including a K-1001HPLC pump, a K-1001 solvent
95 organizer, an on-line degasser, a dynamic mixing chamber and a UV detector K2501 was used for
96 separation and determination of analytes. The separation was performed on the MZ analytical
97 column ODS-3 5 μm (4.6 mm \times 250 mm) with MZ C18 analytical guard column (20 mm \times 4.6
98 mm) packed with the same sorbent under ambient temperature. The solvents used as mobile phase
99 were acetonitrile HPLC-grade and double-distillated water. The analysis was started with 60%
100 ACN with 0.6 mL min^{-1} and after 8:30 min it was increased linearly up to 100% ACN in 4:30 min,
101 at this time flow rate was increased to 1 mL min^{-1} and this percentage and flow rate was maintained
102 until end of the run. The UV detection was performed at 275 nm for imidacloprid, 230 nm for
103 metribuzin and ametryn and 280 for chlorpyrifos. A KDS100 syringe pump (KdScientific Co.,
104 Holliston, MA, US) was used for the polymer solution delivery in the electrospinning process. A
105 Branden-burg (West Midlands, England) regulated power supply was used for electrospinning. The
106 two permanent magnets were NdFeB, model N48 (Ningbo Strong Magnet, China) at the size of 100

107 x 50 x 40 millimeter (mm) and 30 x 30 x 30 mm, respectively. Their magnetic field strength were
108 1.4 and 0.4 tesla, respectively. The morphology and diameter of the fabricated nanofiber sheet were
109 investigated by a TSCAN VEGA II XMU SEM Instrument (Czech Republic).

110

111 **2.2. Reagents and standards**

112 Methanol (HPLC grade), acetone, Iron (III) chloride hexahydrate ($\text{FeCl}_3 \cdot 6\text{H}_2\text{O}$), manganese (II)
113 chloride tetrahydrate and sodium hydroxide (NaOH) were purchased from Merk (Darmstadt,
114 Germany). Nylon 6 (N6) was from Kolon industries Inc. (Korea) and formic acid prepared from
115 Riedel-de Haën (Seelze-Hannover, Germany). Ethyl acetate, 1-Bromodecane and 1-
116 methylimidazole also was purchased from Merk (Darmstadt, Germany). Certified standards of
117 Imidacloprid, metribuzin, ametryn and Chlorpyrifos were supplied from Dr. Ehrenstorfer GmbH
118 (Augsburg, Germany). The stock solution was prepared in methanol at concentration of 1000 mg
119 L^{-1} and stored in refrigerator at 4 °C. A work solution of standard was prepared daily by diluting
120 this solution with doubly distilled water.

121

122 **2.3. Synthesis of Ionic liquid, Decyl-3-Methylimidazolium monobromo-trichloroferrate** 123 **[DeMeIm]-[FeCl₃Br⁻]**

124 Equal molar amounts of 1-bromodecane and 1-methylimidazole were added into a round-bottomed
125 flask fitted with a reflux condenser for about 24 hours at 70 °C with stirring until two phases formed.
126 The top phase layer containing the unreacted starting materials was decanted and removed and then
127 ethyl acetate (a volume approximately equal to half of the bottom phase) was added and followed
128 with mixing. The ethyl acetate was then decanted and the process was repeated two more times to
129 remove the unreacted materials. $\text{FeCl}_3 \cdot 6\text{H}_2\text{O}$ was finally added (equimolar) to DeMeIm and followed
130 by mixing to prepare the desired MIL [DeMeIm]-[FeCl₃Br⁻] (dark brown liquid).

131

132 **2.4. Preparation of electrospun nanofibers**

133 **2.4.1. Primary (unmodified) electrospinning system**

134 The basic electrospinning system was used to prepare the conventional nanofibers. Fig. 1a shows
135 the setup including a horizontal nozzle to Al foil collector configuration. A polymeric solution
136 containing 18% polyamide in formic acid was loaded into the syringe and then electrospayed by
137 applying the DC 15 kV high voltage to two electrodes, the electrospun fibers traveled from the
138 needle (anode) towards aluminium sheet (cathode) in a random mode to prepare the non-woven
139 nanofibers.

140

141 **2.4.2. Auxiliary electrode electrospinning**

142 The auxiliary coiled shape electrode made of copper tube was used as the auxiliary electrode
143 (Fig. 1b). The coil diameter was around 20 cm and distance between the needle tip and aluminum
144 foil collector was set at 15 cm. The negative voltage was connected to the auxiliary electrode was
145 about 5 kV. The assembled set-up was employed to prepare the second type of sorbent by
146 electrospinning of a solution including of 18% polyamide.

147

148 **2.4.3. Magnetic Field Assisted Electrospinning**

149 As Fig.1c shows two permanent magnets were placed in parallel position of the main negative
150 aluminum collector. A solution containing 3% of MIL doped into the 18% polyamide was used to
151 prepare the third sorbent. The electrospinning process was also implemented under the same
152 potential as previously used.

153

154 **2.5. μ -SPE–HPLC analysis of aqueous samples**

155 For μ -SPE device, the prepared nanofibers sheet was removed from the aluminum foil and an
156 amount of 6 mg of sorbent was weighed and cut into small pieces to be packed in the μ -SPE
157 cartridge. Finally μ -SPE cartridge was assembled as the HPLC loop on the six port valve for on-line
158 extraction and preconcentration of the selected analytes. The assembled cartridge was conditioned
159 daily prior to the first extraction by pumping the HPLC mobile phase through it to remove any
160 contaminant and memory effect. It was used for online μ -SPE of imidacloprid, metribuzin, ametryn
161 and chlorpyrifos, as the model analytes, from the aquatic media. Extraction was performed by
162 passing the spiked aqueous samples through the loop. After extraction, the HPLC mobile phase was
163 used for on-line desorption and elution of the extracted analytes from the loop to the HPLC column
164 (Fig. 2). In all experiments, distilled water was spiked with $200 \mu\text{g L}^{-1}$ standards of analytes.

165

166

167 **3. Results and discussion**

168 **3.1. Characteristics and efficiency of the prepared nanofibers**

169 The surface characteristics, diameters and porosity of the prepared nanofibers were investigated by
170 scanning electron microscopy (SEM) technique. As Fig. 3 shows all nanofibers have sufficient
171 homogeneity and porosity while the nanofibers prepared by auxiliary AE and MFAES have more
172 aligned structure. The presence of the pores inside the nanofibers network improved the mass
173 transfer of the analyte throughout the nanofibers and led to the enhanced extraction efficiencies.
174 Although all the prepared nanofibers are favorable for trace analysis but as Fig. 4 shows the
175 MFAES-based nanofibers have dominant extraction properties.

176 The conventional nanofibers have non-woven structure with no regular pattern and a mean diameter
177 of about 600 nm (Fig. 3a and 3b). Reduction in diameters of the nanofibers (about 200 nm) and
178 therefore enhancement in their aspect ratio was achieved when the auxiliary electrode was applied

179 to the spray jet (Fig. 3c and 3d). Auxiliary electrode caused to increase the radical forces in contrast
180 to the total forces toward the collector. For first and conventional nanofibers mat there was just one
181 tensional force toward the collector which is around 1 kV cm^{-1} . In the case of second mat,
182 electrospun under the influence of AE, there were two perpendicular forces including 1 kV cm^{-1}
183 toward the collector (x-axis) and 0.25 kV cm^{-1} radical forces (y-axis). As a result the fibers were
184 whipped more path rather than the conventional mat. This led to an increase in the aspect ratio for
185 the second nanofibers mat in compared with the first one. Comparing the extraction efficiencies of
186 these two nanofibers led to the superiority of the AE assisted nanofibers mat as well. As Fig. 3e and
187 3f show application of MFAES resulted in reduction of nanofibers diameters of the third nanofibers
188 (about 100 nm) in compared with the other two nanofibers. Whipping motion is affected by the
189 solution properties such as conductivity, surface tension, viscosity and also the external forces
190 which can facilitated the jet stretching and result in the reducing the fibers diameters. With
191 introducing the nanofibers in the magnetic field, the charged jet is experienced a radial Lorenz
192 force, and the jet diameter and its direction are affected by the magnetic field gradient. As the
193 nanofibers are spun toward the collector, they are stretched across the gap of two opposite magnetic
194 poles along the directions right angle to the surfaces of the magnets.

195 As ionic liquids increase the ionic conductivity of the solution, addition of MILS cause the
196 reduction in surface tension of polymer solution. The magnetic field can reduce fibers diameter by
197 increasing the velocity of jet and internal alignment of fiber jet. Considering surfactant aspect, the
198 impact of MILS on the surface tension reduction can be more dramatic. With a lower surface
199 tension, the whipping jet is more easily stretched by the electrostatic forces, resulting in smaller
200 fiber diameters. Additionally, fibers are more regular due to a more stable jet that encounters fewer
201 perturbations from the surface tension effect of reducing surface area. Other effects of MILS may
202 be reducing the solvent evaporation rate, thus extending jet stretching and reducing the fiber
203 diameter.

204

205 **3.2. Optimization**

206 After successful preliminary results the synthesized nanofibers mat prepared by MFAES was
207 selected for further optimization and validation. Important and influential parameters including
208 sample flow rate through the loop, the loading time and the sample volume are needed to be
209 optimized to achieve the best conditions. Role of MIL on the extraction efficiency was also
210 essential to be determined. The extraction efficiencies under different experimental conditions were
211 compared using the chromatographic peak area. Moreover, desorption time was also investigated to
212 minimize and/or remove any possible carryover effect. Desorption process must be implemented as
213 quickly as possible to prevent any possible peak broadening. The HPLC mobile phase composition
214 should have sufficient strength for complete desorption of the extracted analytes, while the proper
215 separation of the analytes in the analytical column is kept intact. Considering the selected
216 composition of mobile phase, time duration of 3 min was chosen for prevention of any carryover.
217 Longer desorption times were avoided to maximize the nanofibers sorbent lifetime. All optimizing
218 parameters were performed at the concentration of $200 \mu\text{g L}^{-1}$ using the nanofibers prepared by
219 MFAES.

220

221 **3.2.1. Role of MIL**

222 Magnetic induction of the spray in the field is attributed to the presence of MIL. The charged jet of
223 the sprayed solution containing the doped MIL in polyamide experience a radial Lorentz force, and
224 the jet diameter and its direction are determined by the magnetic field gradient. So, the electrospun
225 nanofibers are more stretched and aligned with lower diameters. The presence of MIL might act as
226 porogens and mediators for the preparation of nanofibers in which more porosity could be formed
227 as well as direct interaction of any remaining of MIL with the target analytes. The MIL amount was

228 therefore investigated from 1% to 20%, and extraction efficiency was increased up to 10% of MIL
229 (Fig. 5a). For further investigation, FTIR spectra from the conventional PA nanofibers, PA-MIL
230 nanofibers and PA-MIL nanofibers washed with water and water/ACN were obtained. As Fig. 6
231 shows, the peak at 3302 cm^{-1} (NH bond) in PA nanofibers was disappeared and replaced with a
232 broad peak for PA-MIL. This is probably due to hydrogen bonding of nitrogen in PA with MIL
233 which consequently led to the observed peak broadening. According to the FTIR spectra, the PA-
234 MIL nanofibers mat contained MIL even after extensive washing with water and water/ACN for
235 several hours. Therefore, it is highly anticipated that MIL could have contributed in the extraction
236 mechanism due to the presence of the decyl group, double bonds and π - π interactions. PA
237 containing 10% of MIL as dopant was selected as the optimum amount for further evaluation of the
238 method.

239

240 3.2.2. Other influential parameters

241 The required time to reach the extraction equilibrium is inversely proportional to the extraction flow
242 rate. The shorter extraction time higher could be achieved at the expense of higher flow rates. In
243 this regard, flow rates of 0.2, 0.5, 1, 2 and 3 mL min^{-1} were investigated and as expected the
244 extraction efficiency was improved as the flow rate of the samples through the SPE cartridge was
245 increased (Fig. 5b). More cycles are passed though the sorbents at a higher flow rate, and therefore
246 greater detection of analytes. The higher flow rates were excluded from the investigation due to the
247 physical limitations.

248

249 The extraction recovery strongly depends on the mass transfer of analyte from sample solution to
250 the extracting nanofibers. The extraction time profile was studied by varying the loading time of the
251 sample solution through the μ -SPE cartridge in the range of 5-35 min. As Fig. 5c shows the
252 extraction efficiency was enhanced as the loading time was increased up to 25 min.

253 The mass of an analyte extracted by the polymeric nanofibers is related to the overall equilibrium of
254 the analyte in the two phases. The overall equilibrium might be also dependent on/independent of
255 the sample volume under the applied conditions. The effect of sample volume was investigated
256 from 5 to 400 mL. As Fig. 5d shows, the extraction efficiency was nearly remained constant for all
257 the used sample volumes and in this study it was independent of sample volume. The mass of
258 analytes extracted by the sorbent is related to the overall equilibrium of the analytes in the two
259 phases. Mass of the analyte extracted by the sorbent is expressed as [24]:

$$260 \quad n = \frac{K_{fs} V_f V_s C_0}{K_{fs} V_f + V_s} \quad (1)$$

261 Equation (1) describes the mass extracted by the polymeric sorbent in equilibrium condition.
262 Clearly, the number of extracted moles “n” is increased as long as sample volume V_s increased,
263 until $K_{fs} V_f \ll V_s$; then, amount of analyte extracted is independent of sample volume:

$$264 \quad n = K_{fs} V_f C_0 \quad (2)$$

265 The effect of sample volume was investigated and varied from 5 to 400 mL. As Fig. 5d shows, the
266 extraction efficiency is independent of sample volume. Apparently at this point the system already
267 reached to the equilibrium and according to equation (2), increasing the sample volume has no
268 effect on the extraction efficiency. Probably equation (1) is valid under pre-equilibrium condition
269 which might be related to the sample volumes lower than 5 mL.

270

271 3.3. Method validation

272

273 Validation of the method was performed by determination of the target analyte based on the
274 optimized conditions, a sampling flow rate of 3 mL min^{-1} , loading time of 25 min, desorption time
275 of 3 min and sample volume of 5 mL. Distilled water spiked with imidacloprid, metribuzin, ametryn
276 and chlorpyrifos was used to evaluate the precision of the measurements, LOD, LOQ, the dynamic

277 range and selectivity of the method. Comparison of chromatograms obtained before (direct injection
278 of 50 μL of 200 $\mu\text{g L}^{-1}$) and after $\mu\text{-SPE-HPLC}$ of the distilled water spiked at 200 $\mu\text{g L}^{-1}$ of the
279 target analytes could be seen in Fig. 7. The linearity of the method was tested by preparing the
280 calibration curve for analyte with 7-10 points. The linearity for the analytes was in the range of 1-
281 500 $\mu\text{g L}^{-1}$. The regression coefficients obtained for all analytes were satisfactory ($R^2 > 0.994$). The
282 values of LOD ($S/N = 3/1$) were in the range of 0.4-4 $\mu\text{g L}^{-1}$ and LOQ ($S/N = 10/1$) 1-10 $\mu\text{g L}^{-1}$.
283 The precision of the method was determined by performing five consecutive extractions from the
284 aqueous solutions at two concentration levels. The standard deviations of the peak area of analyte,
285 spiked at the concentration levels of 20 and 200 $\mu\text{g L}^{-1}$, were satisfactory (Table 1). Caspian Sea
286 and Zayandeh rood river samples were chosen to evaluate the applicability of the developed method
287 in real samples and to investigate the matrix effect. No peaks were observed at the desired retention
288 times of analytes, so they were spiked at two concentration levels of 20 and 200 $\mu\text{g L}^{-1}$. The
289 obtained results proved the robustness of the developed sorbent in real-life sample analysis (Table
290 2).

291

292 4. Conclusion

293 In this project, increasing the aspect ratio of the electrospun nanofibers due to reduction in the
294 diameter resulted in the enhanced extraction efficiency. This was achievable by modifying the
295 primary instrumentation of an electrospinning system via applying some external forces such as
296 auxiliary electrode and introducing some magnets and by addition of material into a polymer
297 solution. Addition of MIL to the solution in MFAES developed system might be helpful to
298 induction the magnetism and also reduction the viscosity and increasing the conductivity of the
299 polymer solution. Improving the conductivity and viscosity of the polymer solution along with
300 surface tension and solvent evaporation rate are some of the reasons for the observed reduction in
301 fiber diameters resulted. The PA polymer jet with higher conductivity, combined with the effect of

302 higher charge repulsion on jet surface due to higher concentration of charges, effectively enhance
303 the jet stretching during whipping and further smaller diameters of the produced nanofibers.
304 Moreover, increasing the MIL effectively improve the extraction efficiency since MIL participate
305 on sorption process. Good extraction efficiency of the prepared sorbent along with its high solvent
306 resistibility and reusability made it so appropriate for trace analysis of target analytes in real
307 samples. The sorbent could be recovered frequently after each subsequent desorption.

308

309

310 **Acknowledgment**

311 The Research Council and Graduates School of Sharif University of Technology (SUT) are thanked
312 for supporting the project.

313

314 **References**

- 315
- 316 [1] H. Bagheri, M. Saraji, *J. Chromatogr. A*, 2001, **910**, 87-93.
- 317 [2] E. Cudjoe, J. Pawliszyn, *J. Pharm. Biomed. Anal.*, 2009, **50**, 556-562.
- 318 [3] Q. Shen, W. Dong, Y. Wang, L. Gong, Z. Dai, H. Cheung, *J. Pharm. Biomed. Anal.*, 2013, **80**,
- 319 136-140.
- 320 [4] H. Bagheri, O. Zandi, A. Aghakhani, *Chromatographia*, 2011, **74**, 483-488.
- 321 [5] H. Bagheri, A. Es'haghi, A. Es-haghi, N. Mesbahi, *Anal. Chim. Acta*, 2012, **740**, 36-42.
- 322 [6] X. Lu, C. Wang, Y. Wei, *Small*, 2009, **5**, 2349-2370.
- 323 [7] J. W. Zewe, J. K. Steach, S. V. Olesik, *Anal. Chem.*, 2010, **82**, 5341-5348.
- 324 [8] H. Bagheri, A. Aghakhani, M. Baghernejad, A. Akbarinejad, *Anal. Chim. Acta*, 2012, **716**, 34-
- 325 39.
- 326 [9] H. Bagheri, A. Aghakhani, M. Akbari, Z. Ayazi, *Anal. Bioanal. Chem.*, 2011, **400**, 3607-3613.
- 327 [10] D. Li, J. T. McCann, Y. Xia, *Small*, 2005, **1**, 83-86.
- 328 [11] P. Katta, M. Alessandro, R. D. Ramsier, G. G. Chase, *Nano Letters*, 2004, **4**, 2215-2218.
- 329 [12] Y. Huang, X. Duan, Q. Wei, C. M. Lieber, *Science*, 2001, **291**, 630-633.
- 330 [13] I. S. Chronakis, *J. Mater. Process. Technol.* 2005, **167**, 283-293.
- 331 [14] R. Murugan, S. Ramakrishna, *Tissue Eng.* 2006, **12**, 435-447.
- 332 [15] D. Li, Y. Wang, Y. Xia, *Nano Lett.* 2003, **3**, 1167-1171.
- 333 [16] D. Yang, B. Lu, Y. Zhao, X. Jiang, *Adv. Mat.* 2007, **19**, 3702-3706.
- 334 [17] T. Welton, *Chem. Rev.*, 1999, **99**, 2071-2084.
- 335 [18] C. Chiappe, D. Pieraccini, *J. Org. Chem.*, 2004, **69**, 6059-6064.
- 336 [19] M. Koel, *Crit. Rev. Anal. Chem.*, 2005, **35**, 177-192.
- 337 [20] G. A. Baker, S. N. Baker, S. Pandey, F. V. Bright, *Analyst*, 2005, **130**, 800-808.
- 338 [21] J. L. Anderson, D. W. Armstrong, G. T. Wei, *Anal. Chem.*, 2006, **78**, 2892-2902.

- 339 [22] J. F. Liu, G. B. Jiang, J. F. Liu, J. A. Jonsson, *TrAC, Trends Anal. Chem.*, 2005, **24**, 20-27.
- 340 [23] E. Aguilera-Herrador, R. Lucena, S. Cárdenas, M. Valcárcel, *TrAC, Trends Anal. Chem.*,
- 341 2010, **29**, 602-616.
- 342 [24] H. Bagheri, H. Piri-Moghadam, A. Es'haghi, *J. Chromatogr. A*, 2011, **1218**, 3952-3957.
- 343
- 344
- 345
- 346
- 347

348

349 **Figures caption**

350 Fig. 1. Schematic diagram of three electrospinning systems. (a) Basic (unmodified) electrospinning
351 system, (b) Auxiliary electrode electrospinning (c) Magnetic Field Assisted Electrospinning

352

353 Fig. 2. On-line μ -SPE-HPLC set-up

354

355 Fig. 3. SEM images of basic electrospinning system (a,b), AES (c,d) and MFAES (e,f) at 3 and 10
356 kX

357

358 Fig. 4. Comparison of the extraction efficiency of the three prepared sorbents, Distilled water was
359 spiked with $200 \mu\text{g L}^{-1}$ of each analyte, Extraction time: 30 min, Flow rate: 3 mL min^{-1} , sample
360 volume: 5 mL

361

362 Fig. 5. Optimization of the influential parameters on the extraction efficiency. (a) MIL percentage,
363 (b) Sample flow rate, (c) Loading time, (d) Sample volume. Distilled water was spiked with $200 \mu\text{g}$
364 L^{-1} of each analyte.

365

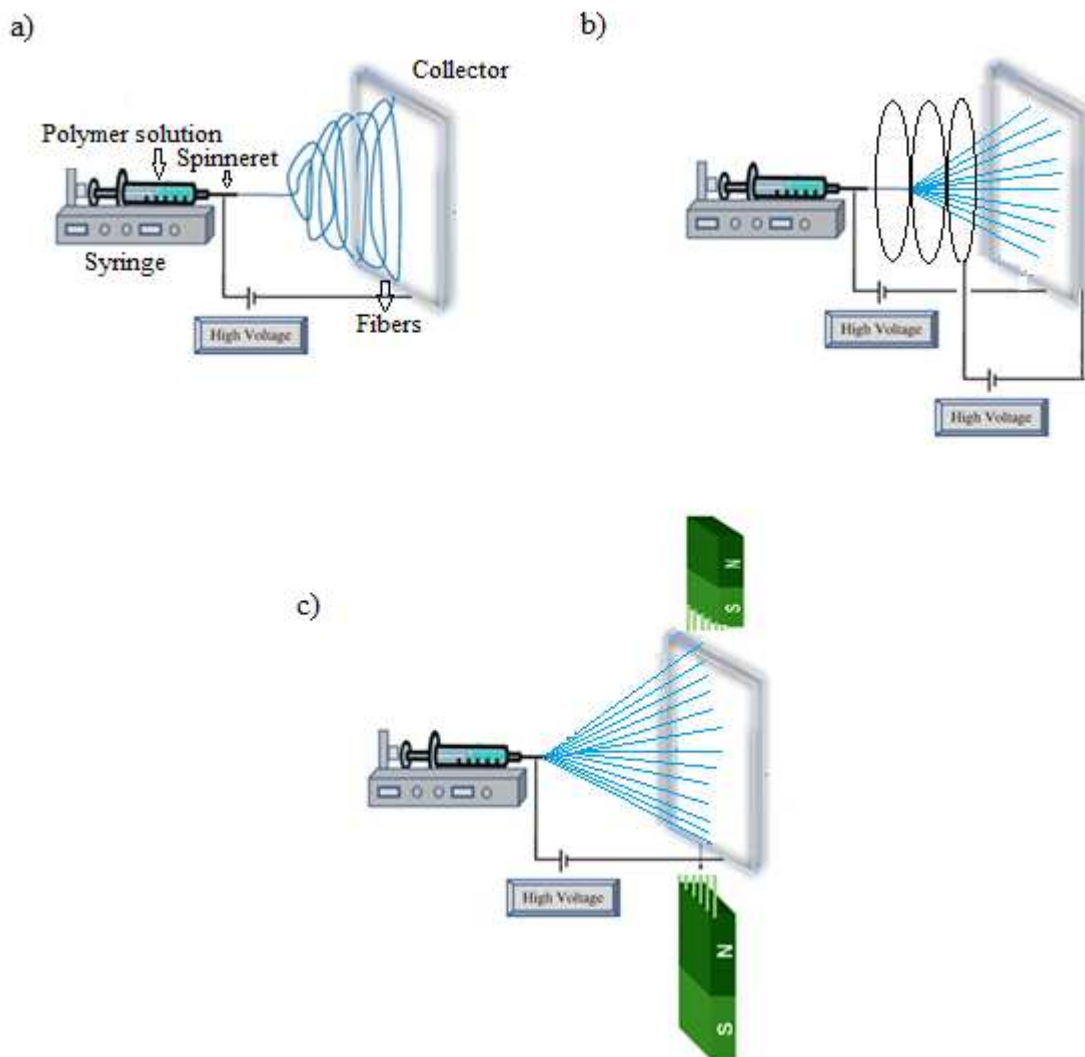
366 Fig. 6. The IR spectra from the electrospun a) PA-MIL washed with H_2O and $\text{H}_2\text{O}/\text{ACN}$, b) PA-
367 MIL c) PA

368

369 Fig. 7. Chromatograms obtained by on-line μ -SPE HPLC of the target analytes, before (direct
370 injection) and after μ -SPE of the spiked distilled water with the analytes at concentration of $200 \mu\text{g}$
371 L^{-1} . Imidacloprid, metribuzin, ametryn and Chlorpyrifos are eluting respectively.

372

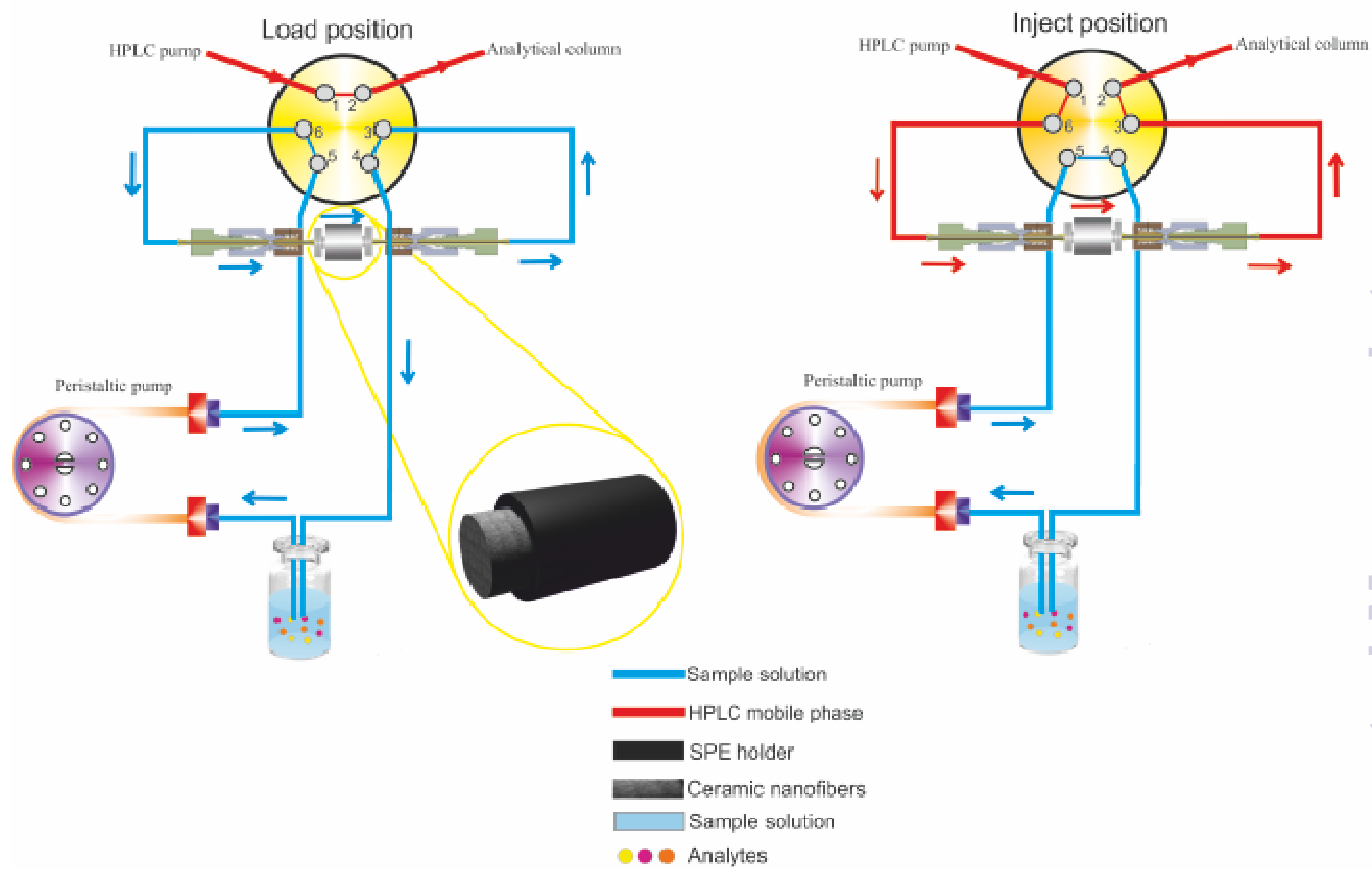
373 Fig. 1
374



375
376

377
378
379
380
381
382
383
384
385
386
387
388
389

390 Fig. 2
391



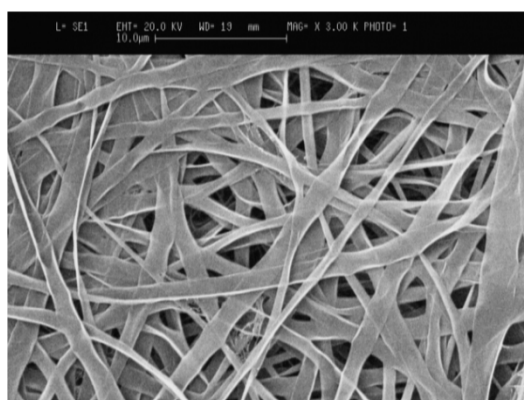
392
393
394
395
396
397

398
399 Fig. 3
400

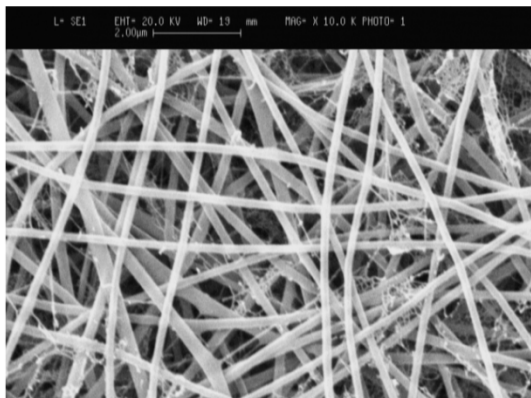
a)



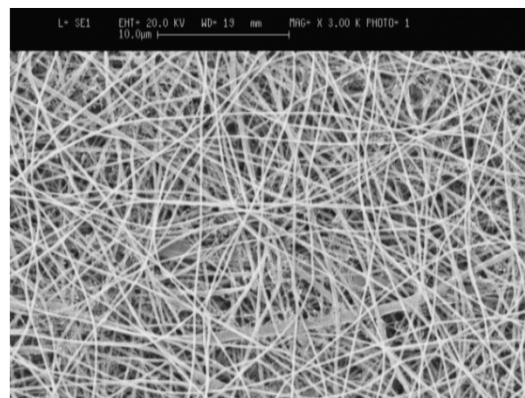
b)



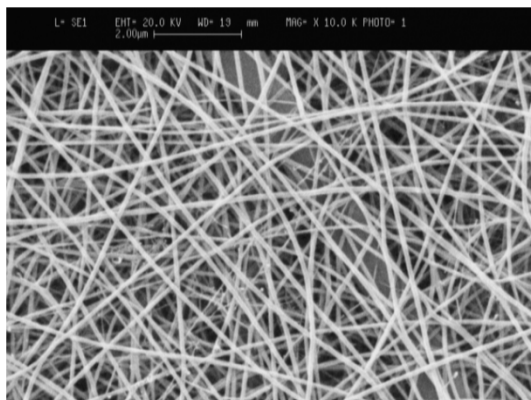
c)



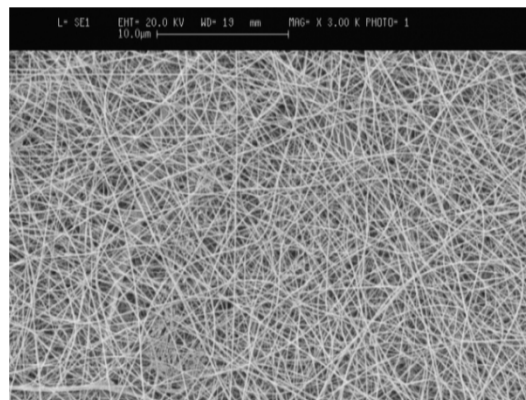
d)



e)

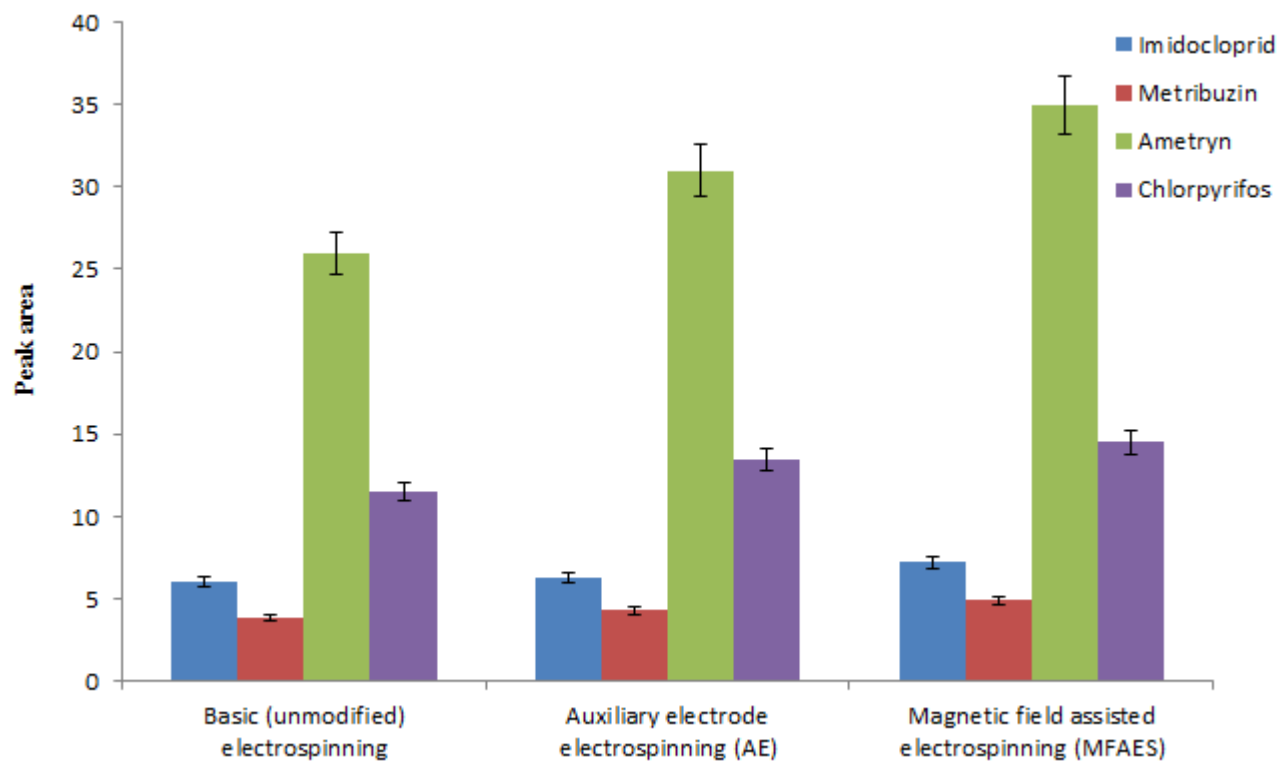


f)



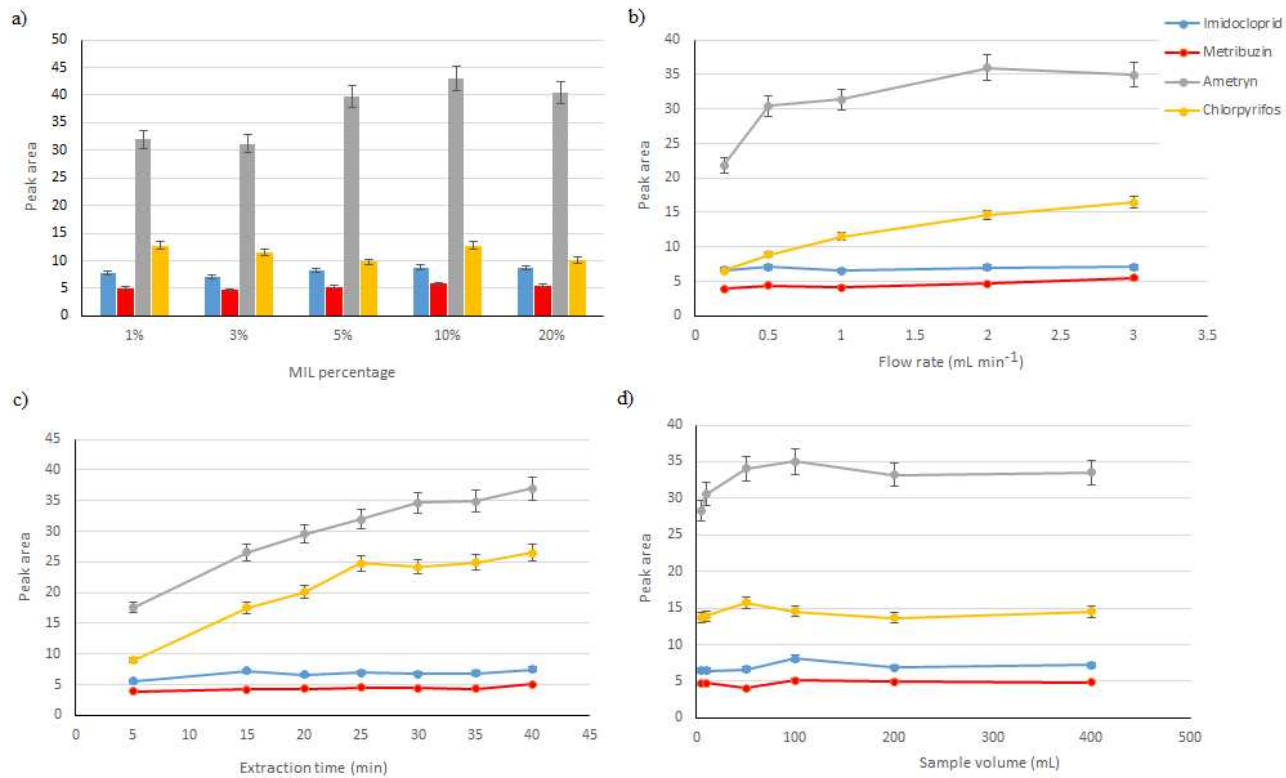
401
402

403 Fig. 4
404
405
406



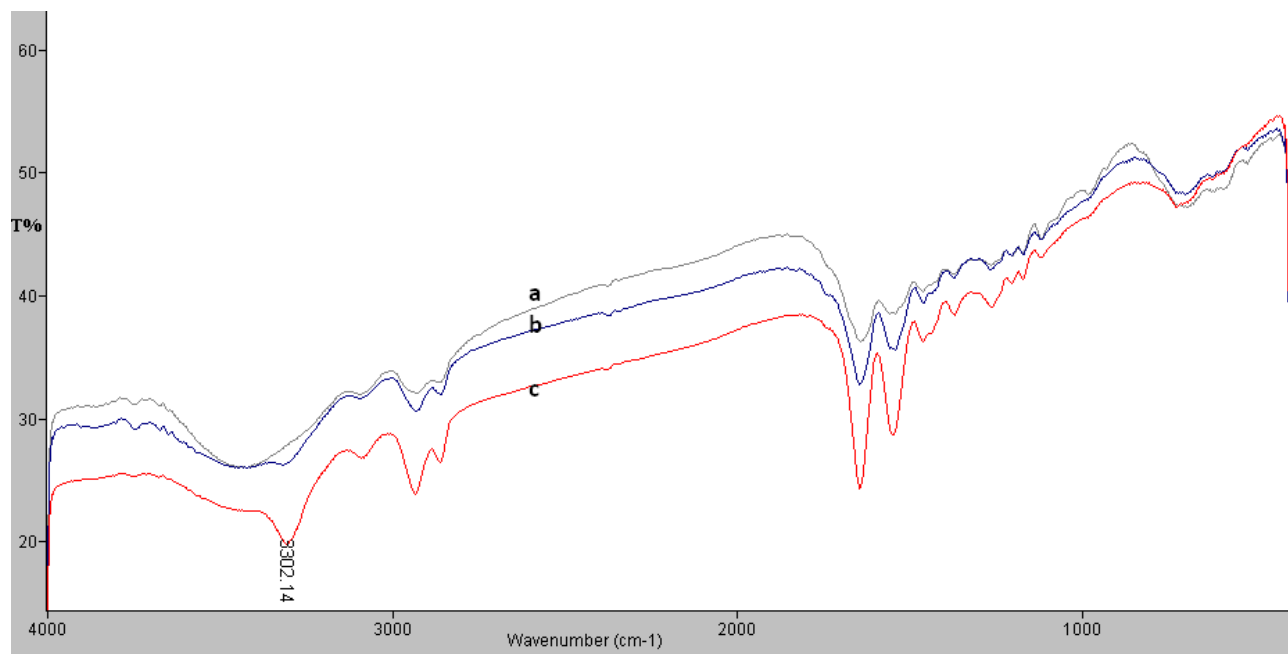
407
408

409
410 Fig. 5
411
412
413
414
415



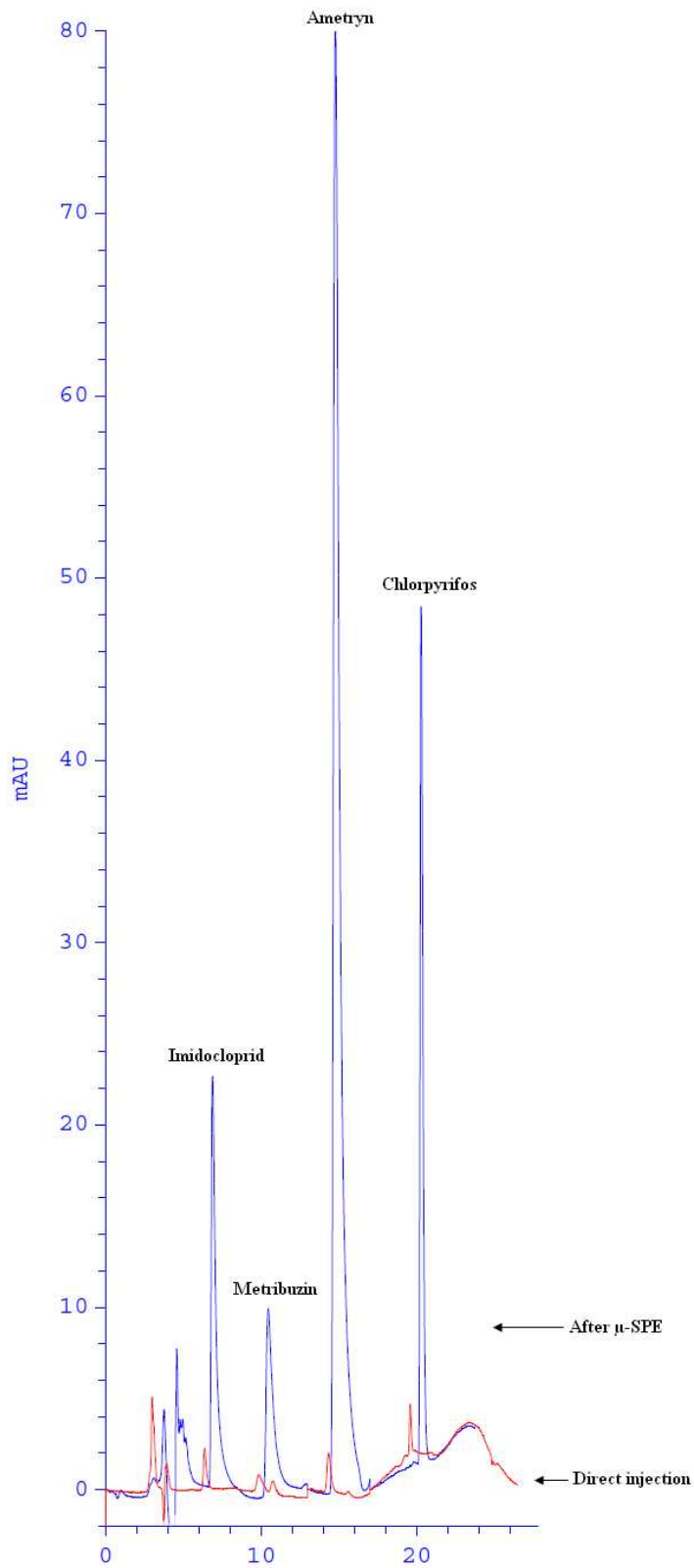
416

417
418 Fig. 6
419
420
421



422
423

424 Fig. 7
425



RSC Advances Accepted Manuscript

426
427
428
429

430

431 Table 1- Figures of merit of the method

Compounds	LDR ^a ($\mu\text{g L}^{-1}$)	LOD ^b ($\mu\text{g L}^{-1}$)	LOQ ^c ($\mu\text{g L}^{-1}$)	R ²	Regression equation	RSD% (n=5) ^d	RSD% (n=5) ^e
Imidacloprid	5-500	2.0	5.0	0.9962	$y = 0.0295x - 0.2856$	10.5	3.8
Metribuzin	10-500	4.0	10.0	0.9941	$y = 0.0185x - 0.1906$	5.9	3.4
Ametryn	1-500	0.40	1.0	0.9987	$y = 0.2584x + 0.63$	7.3	4.8
Chlorpyrifos	3-500	1.0	3.0	0.9946	$y = 0.0691x - 0.3222$	11.5	3.9

432 ^a Linear dynamic range433 ^b S/N=3434 ^c S/N=10435 ^d C_{analytes}=20 $\mu\text{g L}^{-1}$ 436 ^e C_{analytes}=200 $\mu\text{g L}^{-1}$

437

438

439

440

441

442

443

444
 445 **Table 2**
 446
 447
 448
 449 Relative recoveries for real samples spiked with the selected analytes at two concentration levels
 450

Analyte	Zayandeh rood river				Caspian Sea			
	RR % ^a	RSD % (n=3) [*]	RR % ^b	RSD % (n=3) ^b	RR % ^a	RSD % (n=3) ^a	RR % ^b	RSD % (n=3) ^b
Imidacloprid	91	8.9	96	6.1	87	11.5	91	8.3
Metribuzin	103	8.4	95	5.4	85	9.1	93	9.1
Ametryn	108	10.3	103	5.6	104	10.4	98	8.9
Chlorpyrifos	105	10.1	92	8.8	97	11.4	107	5.5

451 RR: Relative Recovery

452 ^aC_{analytes} = 20 µg L⁻¹

453 ^bC_{analytes} = 200 µg L⁻¹

454

455

456

457

458

459